

# MIDFIELD RF SIGNAL DETECTOR

by

Dawei Zhang

Senior Project

Electrical Engineering Department

California Polytechnic State University

San Luis Obispo

Dec 2015

## Abstract

The project goal is to design a RF signal detector specialized for measuring the received signal level from 1.6GHz midfield wave. Midfield waves match impedance of a human body and allow signals to deteriorate less when traveling through flesh. This technology was initially developed at Stanford to recharge the battery of implanted device but is used in this project to detect changed in blood composition. The output of the sensor is a two digit voltage level indicating the RSSI (Received Signal Strength Indicator).

## TABLE OF CONTENTS

Abstract.....	2
Acknowledgement.....	6
1. Introduction.....	7
2. Background.....	8
3. Requirements and Specifications.....	10
3.1 Band Pass Filter Design.....	11
3.2 Mixer PCB board design.....	16
3.3 LT5534 specification.....	17
4. Construction.....	19
5. Testing.....	21
5.1 Test Setup.....	21
5.2 Test Results .....	22
6. Conclusions and Recommendations.....	27
7. Bibliography.....	28

LIST OF TABLES	page
Table 3.1 Summary of Prototype Filter Transformation.....	12
Table 3.2 Fifth order bandpass filter stub design.....	15
Table 3.2 LT5534 RF detect sensitivity and range design.....	18

LIST OF FIGURES	page
Figure 3.1 LT5534 RF detector validation test plan.....	10
Figure 3.2 Bandwidth of Band Pass Filter.....	11
Figure 3.3 An example of second order band pass filter.....	12
Figure 3.4 Quarter wave length transmission line.....	13
Figure 3.5 quarter-wave-length stubs second band pass filter and its equivalent circuit.....	14
Figure 3.6 Second order band pass filter equivalent circuit .....	14
Figure 3.7 Fifth-order band pass filter ADS schematic.....	15
Figure 3.8 1.6GHz band pass filter ADS layout.....	16
Figure 3.9 ADE_42MH mixer matching circuit layout .....	17
Figure 3.10 LT5534 datasheet received power vs output DC voltage.....	18
Figure 4.1 Mixer FR4 PCB board.....	19
Figure 4.2 Band pass filter with five short stubs.....	20

Figure 5.1 Test bench set up.....	20
Figure 5.2 ADE mixer output signal spectrum.....	22
Figure 5.3 ADS simulation and measured band pass filter $S_{21}$ performance.....	23
Figure 5.4 BPF filters out unwanted frequencies at 400MHz and out-of-band harmonics.....	24
Figure 5.5 Spectrum analyzer midfield power measurement from 1.3 to 1.9GHz.....	25
Figure 5.6 LT5534 RF Detector output DC voltage vs. received power.....	26
Figure 5.7 RSSI reading on LCD screen using Arduino Uno board.....	26

## Acknowledgement

I really appreciate Dr. Smilkstein's time and guidance on my project. I also want to thank Jason Schray and Danielle Nishida's constant support and teamwork during in the project. Finally I want to thank Cal Poly EE department for providing all testing equipment and software design tool as well as milling workshop to make the project Design – Manufacture – Validation - Operation process possible.

## 1. Introduction

This project is part of a Master's thesis [10] which looks at alternative ways to measure blood glucose. The Master's thesis uses mid-field signals in order to match impedance and therefore lose less power as they travel through flesh. The goal of this senior project is to build a receiver for those signals and give accurate RSSI (received signal strength indicator) measurements. Mid-fields were originally explored by Stanford professor Dr. Ada Poon [3] who used the signaling technique to recharge the batteries of deeply implanted devices. Devices implanted near the surface of the skin were able to have their batteries recharged using inductive coupling but when devices were implanted deeper in the body, the drop in energy before the signals reached the devices made wireless recharging impractical. Using inductive coils to transmit energy is a near field application and the near field coupling decays as  $1/d^3$  from the source [1]. Far field transmission is called radiative mode when it is used for far field power transfer, and the power decays as  $1/d^2$ , which can be used when the implant is much smaller than its distance from the source. Dr. Poon discovered how to match impedances with flesh which allowed signals to travel farther without attenuation. These signals are called mid-field signals and occupy a position between near field and far field signals. Poon et al showed that in the midfield power transfer combines inductive and radiative modes [2] and shows much less attenuation as it travels through the body. The project described in this report is part of the larger glucose sensor project but because the glucose sensor system may be patented in the future, details of the work will not be described here. The glucose sensor system needs to sense the strength of a 1.6GHz mid-field wave at some point in the system and developing a sensor to receive and measure RSSI is what is described in this project.

In chapter 2 the background of implanted medical devices and midfield mathematical details are presented. Chapter 3 describes midfield validation test components and requirements. Chapter 4 describes the project components and construction. In chaapter 5, the midfield testing results are analyzed.



## 2. Background

Traditionally short distance wireless communication is done by inductively coupling using inductive coils. The near field inductively coupling basis of power transfer is Faraday's law at frequency  $\omega$

$$V = i\omega\mu_o \int H \cdot ds \quad (2.1)$$

Where H is the electromagnetic field created by the source and V is the inducted voltage on the receiver. The inductively coupling has an advantage of low signal loss passing through biological structures such as flesh. However, the inductively coupling behaves in near field coupling which decays in  $1/d^3$ , and the power transfer efficiency is really low for a millimeter size devices to coupling devices through the thickness of a flesh.

The midfield powering does not use the conventional inductively coupled coils. Instead it uses a patterned metal plate to transmit energy through the flesh. The challenge is to simulate the flesh structure and impedance matching to the flesh. The signal power received by the receiver needs to be measured to validate the midfield transmitting device, thus the path loss through the flesh can be numerically calculated by taking the transmitted power and subtracting the received RSSI.

For mm-microwave devices, the transfer efficiencies are obtained by midfield powering are -30dB to -40dB in general. It makes the midfield powering method for tiny, low-power devices with power consumption in the milliwatt to microwatt range. A midfield powering system can transmit RF signal at 30dBm, which is within the FCC regulation. Consequently, after the transmitted midfield signal passes the flesh and received by the devices, it can provide the devices sufficient power (-30dBm to -40dBm) to function. And the RF detector system is used to validate the actual RSSI at the receiving device.

### 3. Design decisions and construction

The project includes the following components: A mixer, band pass filter, RF signal detector, and Arduino Uno board. In the project, a signal is transmitted from a source and that signal will be detected and measured on the receiver side as DC voltage which is displayed as the signal's RSSI level.

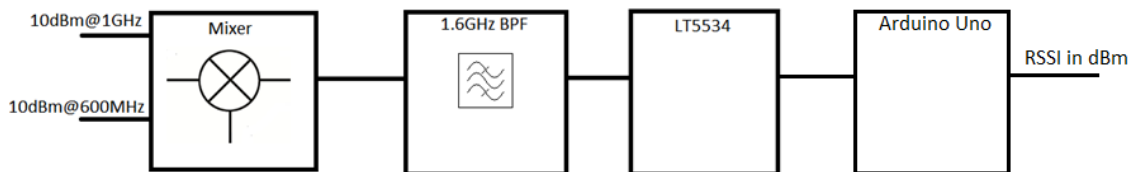


Figure 3.1 LT5534 RF detector test plan

Figure 3.1 shows the block diagram of the RF signal detector validation test plan. The midfield power signal centers at 1.6GHz so a 1.6GHz CW (continuous wave) tone is generated as the arbitrary test signal. Since the school microwave lab RF signal generator can only provide a RF signal up to 1GHz frequency, a mixer is required to produce a 1.6GHz CW tone. Due to the mixer's linearity and non-linearity, an image signal at 0.4GHz and harmonics are produced. A band pass filter centered at 1.6GHz is needed to eject out-of-midfield band signals to make sure the RF detector only detects the signal at 1.6GHz. Once the RF signal's RSSI has been detected, it is processed and displayed through by Arduino Uno. Details of each of these blocks are described in this chapter.

### 3.1 Band Pass Filter

A bandpass filter can be treated as a low pass filter with a corner frequency at  $\omega_2$  and a high pass filter with a corner frequency at  $\omega_1$ , and the conversion to a bandpass filter is accomplished with

$$\omega = \frac{1}{\Delta} \left( \frac{\omega}{\omega_o} - \frac{\omega_o}{\omega} \right) \quad (3.1)$$

where

$$\Delta = \frac{\omega_2 - \omega_1}{\omega_o} = 0.2 \quad (3.2)$$

is the normalized bandpass filter bandwidth:

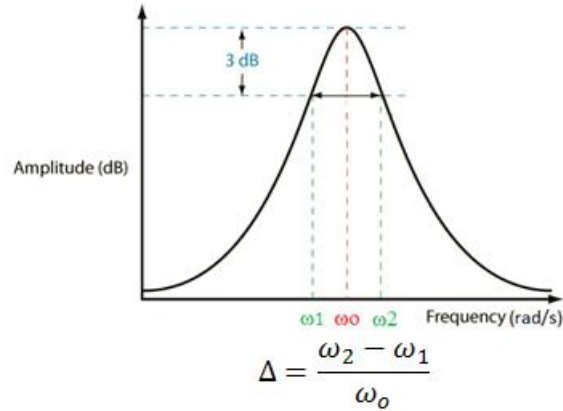


Figure 3.2 Bandwidth of Band Pass Filter

$Z_L = j\omega L$  can be substituted into Equation 3.1 to get:

$$Z_L = j \frac{1}{\Delta} \left( \frac{\omega}{\omega_o} - \frac{\omega_o}{\omega} \right) L = j\omega \frac{L}{\omega_o \Delta} + \frac{1}{j\omega} \frac{\omega_o L}{\Delta} \quad (3.3)$$

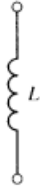

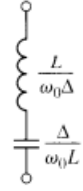
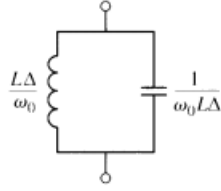
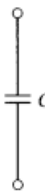

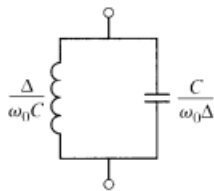
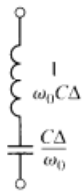
$Y_c = j\omega C$  can be substituted into Equation 3.1 to get:

$$Y_c = j \frac{1}{\Delta} \left( \frac{\omega}{\omega_o} - \frac{\omega_o}{\omega} \right) C = j\omega \frac{C}{\omega_o \Delta} + \frac{1}{j\omega} \frac{\omega_o C}{\Delta} \quad (3.4)$$

Table 3.1 shows prototype filter transformations, and the bandpass filters can be accomplished by using either series LC or parallel LC.

Table 3.1 summarizes these transformations:

Table 3.1 Summary of Prototype Filter Transformations

Low-pass	High-pass	Bandpass	Bandstop
			
			

$\Delta = \frac{\omega_2 - \omega_1}{\omega_0}$

As mentioned earlier, a quarter-wave-length open circuit stub = series resonant circuit and a quarter-wave-length short circuit stub = parallel resonant circuit. In Figure 3.3, when a series of resonant circuits are interconnected by impedance inverters, a band pass filter model can be achieved:

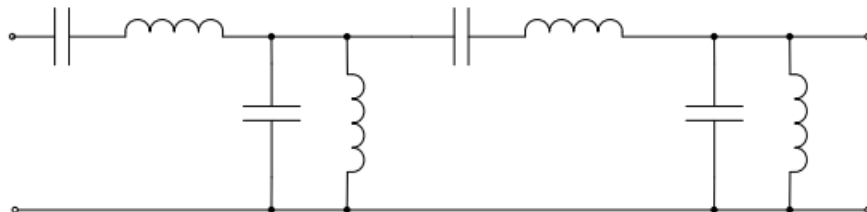


Figure 3.3 an example of a second order band pass filter

Figure 3.4 shows the quarter wave length transmission lane:

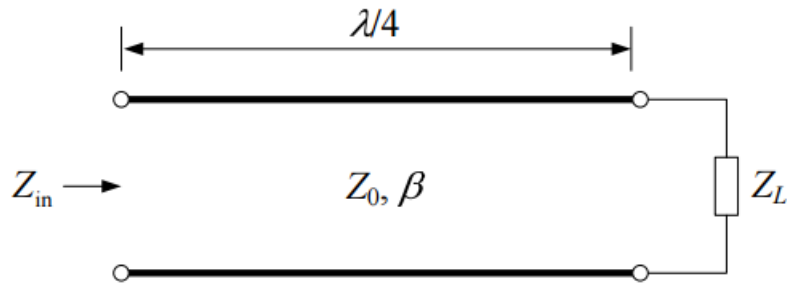


Figure 3.4 Quarter wave length transmission lane

The normalized input impedance is the inverse of the normalized load impedance  $Z_{in} = \frac{Z_0^2}{Z_L}$

Taking the second order band pass filter as an example, the quarter wave length long, short stubs are used to construct the second order band pass filter, as shown in Figure 3.5. The quarter-wave-length series stub with impedance  $Z_0$  plays the role of the impedance inverter. Looking from the source on the left port, the equivalent band pass filter is shown in Figure 3.6.

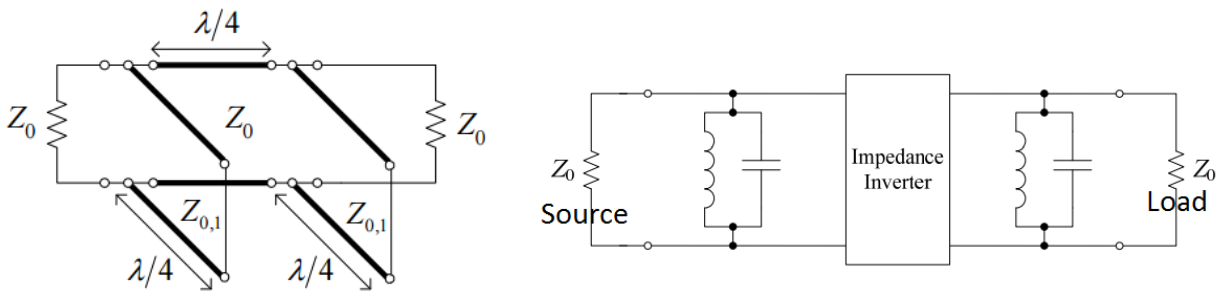


Figure 3.5 quarter-wave-length stubs second band pass filter and its equivalent circuit

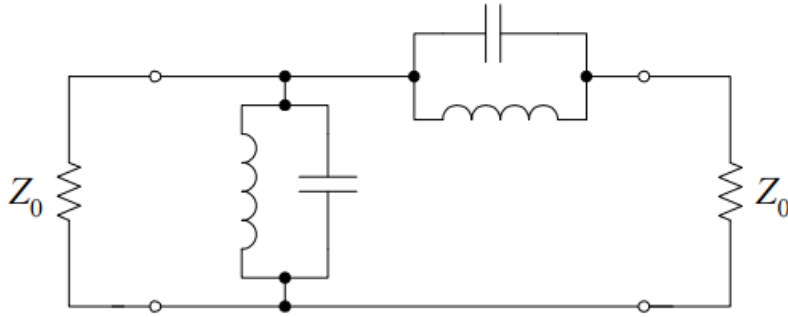


Figure 3.6 second order band pass filter equivalent circuit

The impedance of each stub can be calculated using the equation [8]:

$$Z_{0n} = \frac{\pi * Z_0 * \Delta}{4 * g_n} \quad (3.5)$$

Table 3.2 shows a fifth order band pass filter. The higher order the band pass filter is, the steeper roll off slope the band pass filter will have; however the tradeoff is more ripples on the edge, which will result in a fluctuating BPF insertion loss. Therefore, the RSSI reading would be inaccurate. So fifth order is the moderate design which involves the consideration of roll off slope and pass band ripple.

Table 3.2 Fifth order bandpass filter stub design

n	g <sub>n</sub>	Z <sub>0n</sub> (Ω)
1	2.135	3.67868
2	1.0911	7.198223
3	3.001	2.617122
4	1.0911	7.198223
5	2.135	3.67868

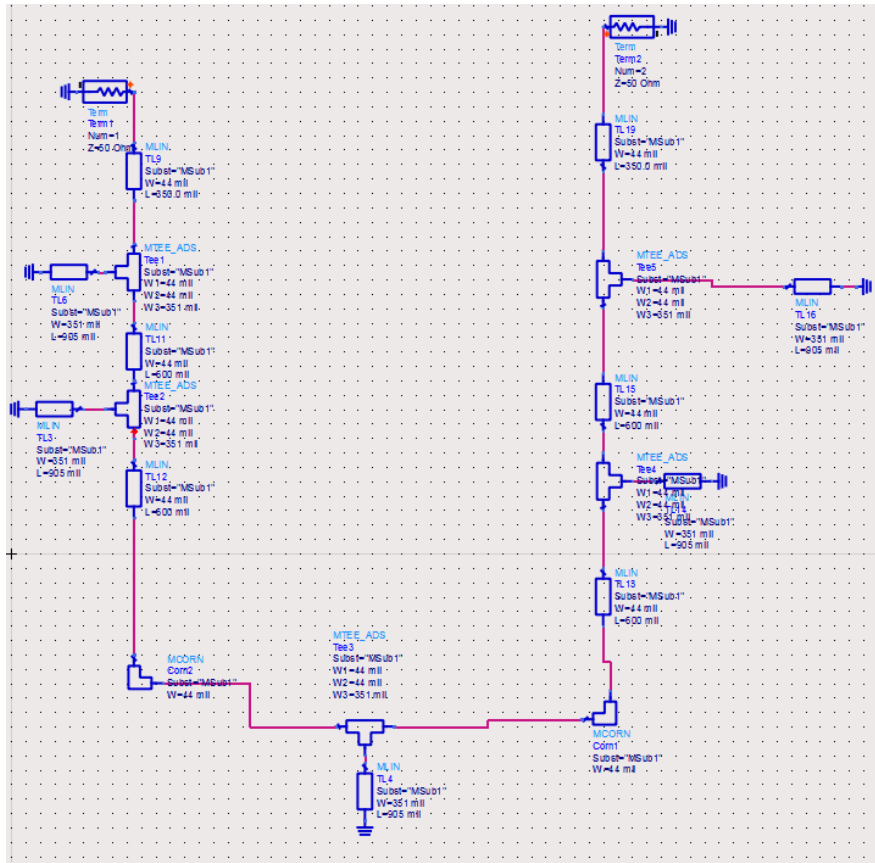


Figure 3.7 Fifth-order BPF schematic

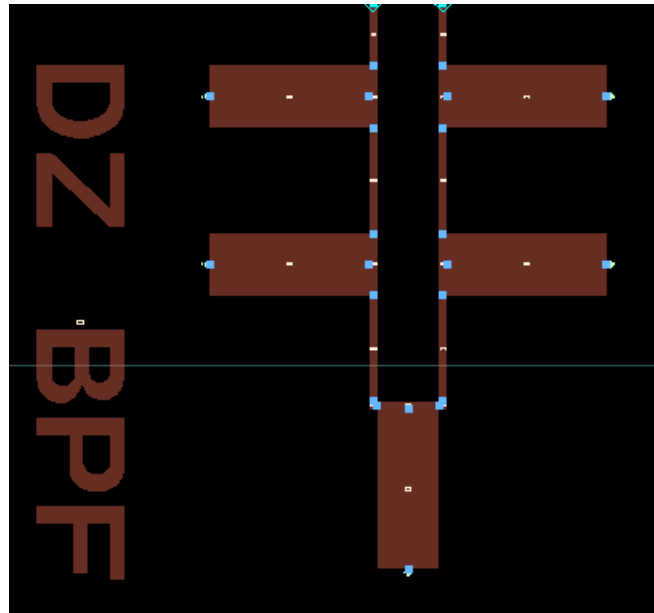


Figure 3.8 1.6 GHZ BPF Design layout

### 3.2 Mixer PCB board design:

A SIM-U432H+ mixer IC chip is chosen for the project because:

1. IF (IN) port is from 0.1 – 800MHz, which can take the 600MHz input IF frequency from the RF signal generator at school. And it is an UP converter frequency mixer, which is what the project requires.
2. The IC chip outline transmission lane width minimum size is 25mil, which is larger than the school milling machine threshold 20mil.
3. The conversion loss is 7.5dB and IP3 is 26dBm, which sets the mixer compression point.

The harmonics are used to validate the 1.6GHz band pass filter.

Figure 3.9 shows the mixer advanced design system PCB layout design. Transmission line widths are carefully selected. Note that ground pad design is not finished, more grounding techniques will be discussed in section 4.





Figure 3.9 ADE\_42MH mixer matching circuit layout

### 3.3 LT5534 specification

Table 3.3 is the datasheet of the IC chip LT5534. LT5534 is used to detect RSSI from 0 to -60dBm for a RF frequency range of 50MHz to 3GHz. In addition, the RF signal in a decibel scale is converted into DC voltage linearly in both 50MHz to 900MHz frequency range and 900MHz to 3GHz frequency range, and the precision is up to 2 decibels. Moreover the latency for the output respond is less than 40ns, which is negligible for our application.

Table 3.3 LT5534 RF detect sensitivity and range

<b>ELECTRICAL CHARACTERISTICS</b> $V_{CC} = 3V$ , $EN = 3V$ , $T_A = 25^\circ C$ , source impedance = $50\Omega$ , unless otherwise noted. Test circuit shown in Figure 1. (Note 2)					
PARAMETER	CONDITIONS	MIN	TYP	MAX	UNITS
<b>RF Input</b>					
Frequency Range			50 to 3000		MHz
Input Impedance			2		k $\Omega$
<b><math>f_{RF} = 50MHz</math></b>					
RF Input Power Range			-58 to +2		dBm
Dynamic Range (Note 3)	$\pm 3dB$ Linearity Error, $T_A = -40^\circ C$ to $85^\circ C$		60		dB
Output Slope			44		mV/dB
Output Variation vs Temperature	$P_{IN} = -48dBm$ to $-14dBm$ , $T_A = -40^\circ C$ to $85^\circ C$		0.007		dB/ $^\circ C$
<b><math>f_{RF} = 900MHz</math></b>					
RF Input Power Range			-60 to 0		dBm
Dynamic Range (Note 3)	$\pm 3dB$ Linearity Error, $T_A = -40^\circ C$ to $85^\circ C$		60		dB
Output Slope			41		mV/dB
Output Variation vs Temperature	$P_{IN} = -48dBm$ to $-14dBm$ , $T_A = -40^\circ C$ to $85^\circ C$		0.008		dB/ $^\circ C$

Figure 3.10 shows the chip LT5534 DC output voltage vs RSSI as RSSI varies from 0 to -60dBm at 900MHz. The temperature variation is less than 1% for its RSSI varies from -10 to -50dBm. The specification was validated and the results are presented in section 5.

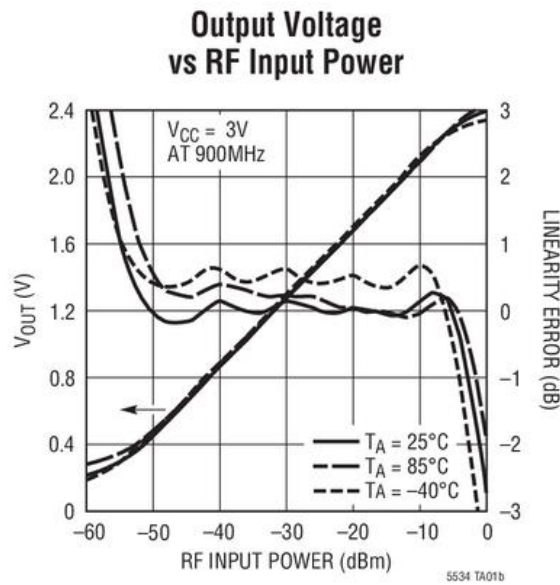


Figure 3.10 LT5534 datasheet received power vs output DC voltage [2]

#### 4. Construction

Figure 4.1 shows the two-layer mixer PCB board. RF, IF and LO ports are labeled and soldered with a female SMA connectors. Both ground pads in left and right are drilled through and soldering shorted with the ground on the PCB back layer. There are dielectric and parasitic inductance and capacitance in RF frequencies, a good grounding around the RF circuitry can minimize it.

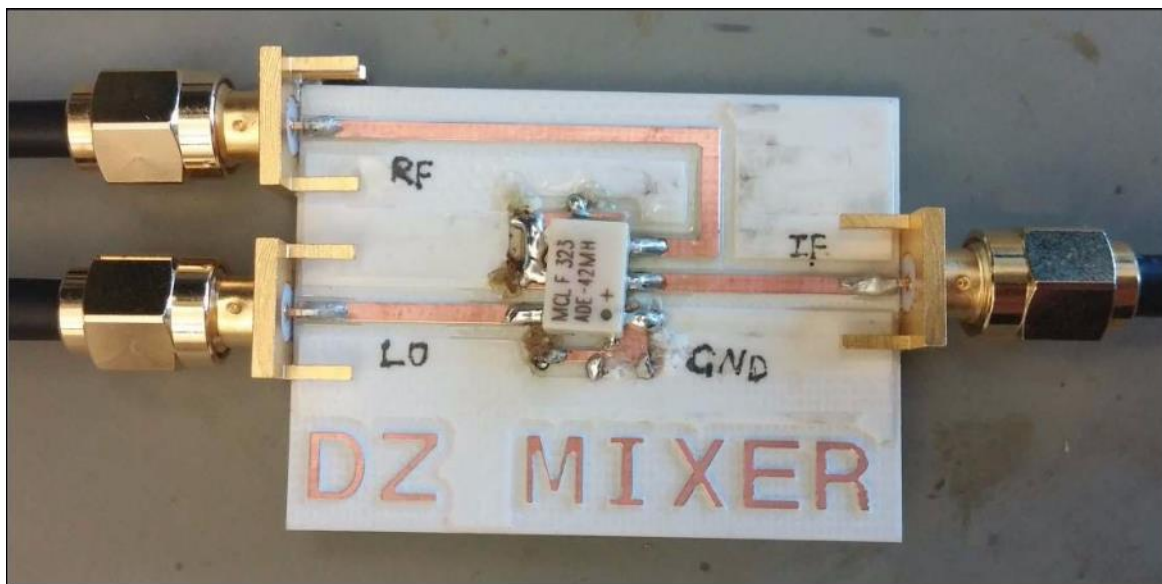


Figure 4.1 Mixer FR4 PCB board

Figure 4.2 shows the fifth order band pass filters designed with five short stubs. Note that the end of each quarter-wave-length shunt stubs are drilled through and connected to the back layer ground as short stubs. The quarter-wave stubs are “open” at 1.6GHz midfield band, and “short” at out-band frequencies. The design was made on Advanced Design System (ADS) simulation software. The measurement showed a -1.7dB loss at pass band, and a -62dN rejection in the

outside-band, which will fulfil the goal of rejecting the unwanted signal at 400MHz and harmonics.

Both mixer and BPF were milled in Cal Poly workshop and a detailed milling machine user manual was wrote as well for future users and courses.

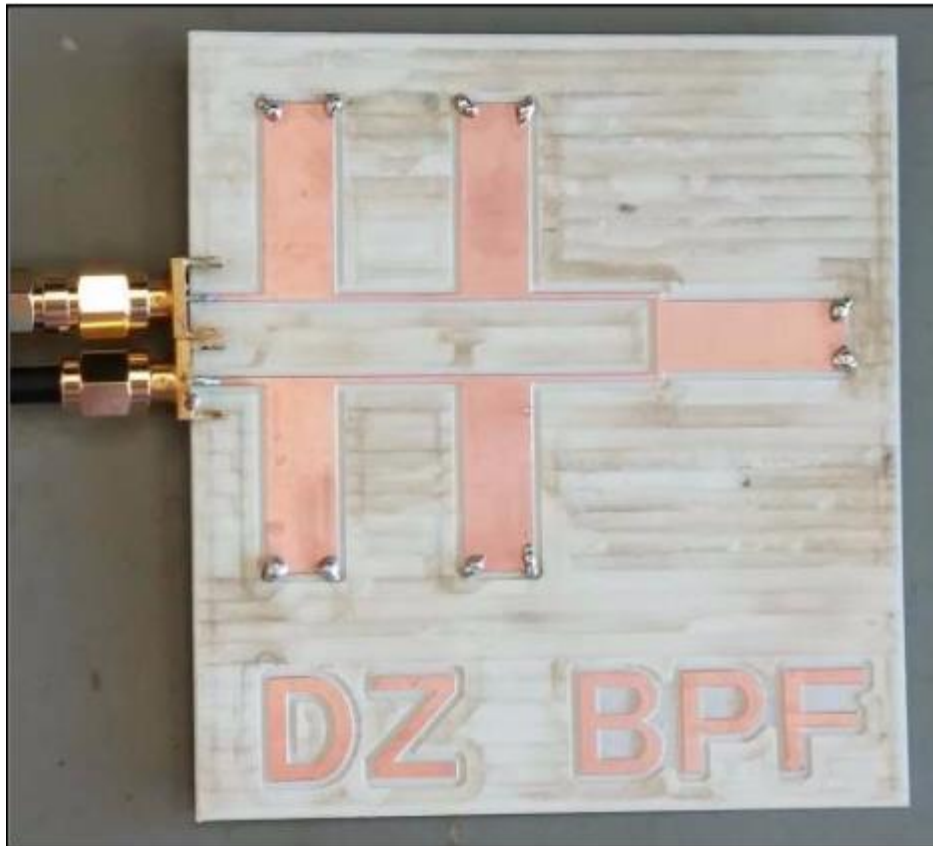


Figure 4.2 Band Pass Filter with five short stubs ( $f_0=1.6\text{GHz}$ )

## 5. Testing

In this section the test set-up and test results will be described.

### 5.1 Test Setup

The power of our midfield signal needs to be precisely detected and read on the receiver side. Also a real-life full system test is required for validation. To do that, a mixer is used as the arbitrary midfield signal generator. The mixer generates the 1.6GHz signal which is then filtered by the fifth order band pass filter (BPF) to get rid of the out-of-band signals and then feed into the RF signal detector. A DC voltage is read by LT5543 and it outputs the DC voltage to the Arduino Uno board. The Arduino Uno board linearly converts the DC voltage back to the RSSI in unit of dBm, and then the RSSI is displayed on the LCD board using a properly adjusted voltage divider.

Figure 5.1 shows the RF signal detector validation test set up.

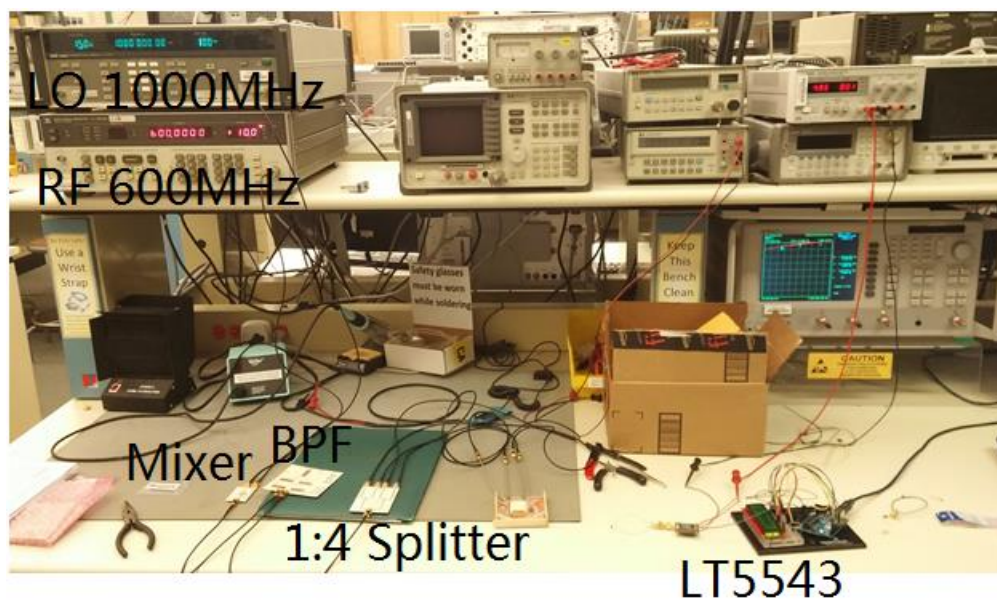


Figure 5.1 Test bench set up

## 5.2 Test results

Figure 5.2 shows the mixer output signal when a 10dBm RF signal at 600MHz mixes with a 10dBm LO signal at 1GHz. On the spectrum analyzer, a -5.54dBm signal sits at 1.6GHz, and an unwanted -4.2dBm signal sits at 400MHz as well. The RF detector also reads an RF signal from 50MHz to 900MHz with a linear scale of 44mV/dB, and the harmonics at 1GHz and 2GHz are only 12dB less than the 1.6GHz signal. If the mixer output signal is directly connected to the RF detector, the RSSI will convert them all in DC voltage, which not give the results desired of the actual midfield power level.

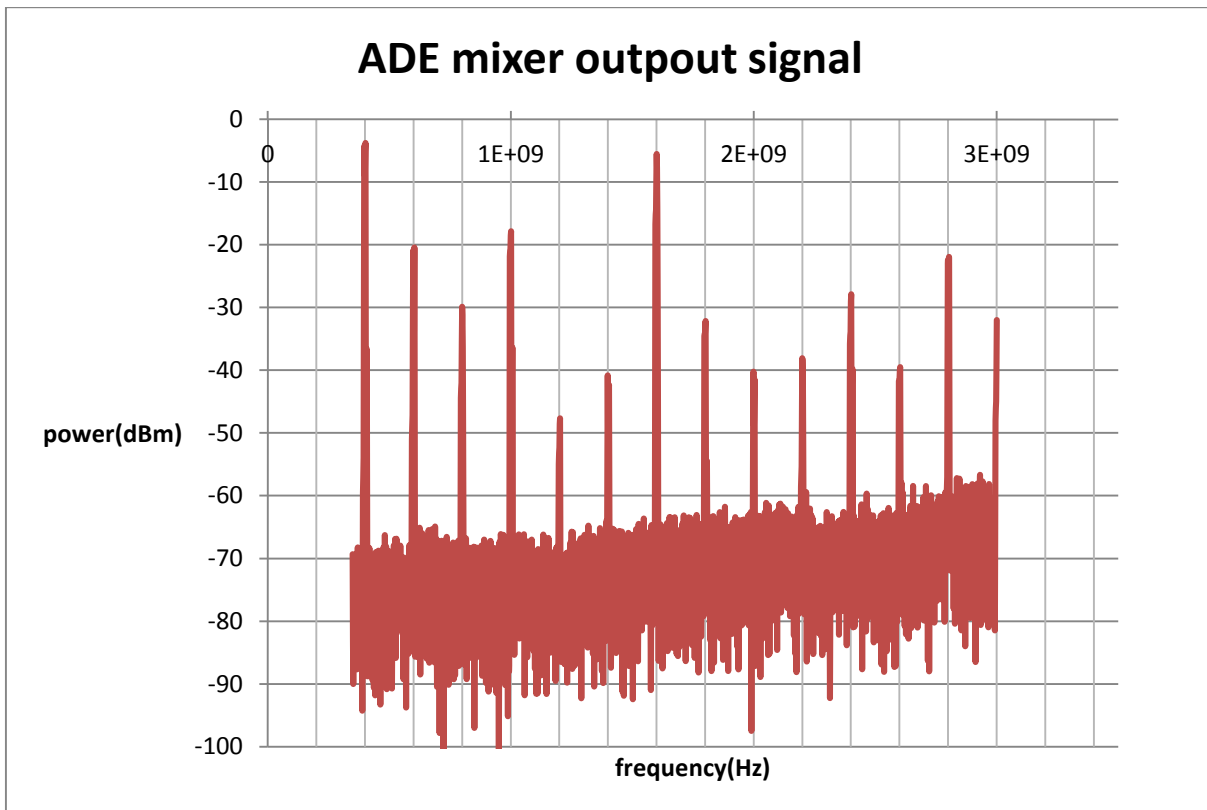


Figure 5.2 ADE mixer output signal spectrum

To avoid the unwanted signals generated by the mixer due to its non-linearity, only the mixer output signal at 1.6GHz is allowed to be used as input to the LT5534. In figure 5.3, a BPF centered at 2GHz is simulated. The reason to choose 2GHz-centered band-pass filter is that in the previous design the BPF simulated at 1.6GHz, but the fabricated BPF actually was centered at 1.2GHz. As a result, the fabricated BPF (which theoretically was centered at 2GHz) actually is centered at 1.6GHz with 1.7dB insertion loss, which meets the 2dB insertion loss specification.

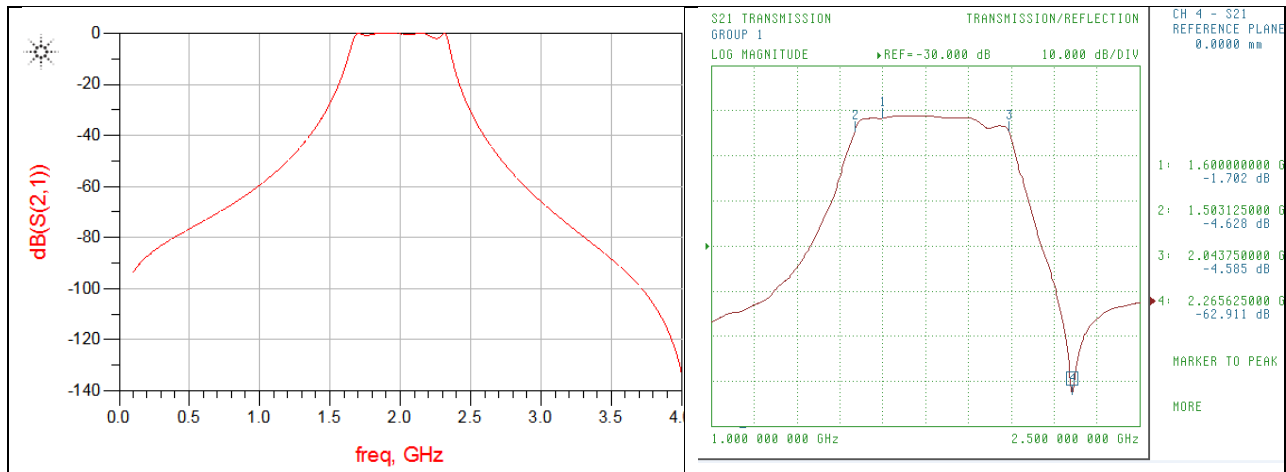


Figure 5.3 ADS simulation and measured BPF S21 performance

In figure 5.4, the blue lines represent the filtered ADE\_42MH mixer output signal after it has been passed through the 1.6GHz BPF. On the output stage of the BPF, a -8.2dBm signal is at 1.6GHz and 2 harmonics are at 1.8GHz and 2GHz; and the harmonics are at least 30dB lower than the -8.2dBm signal. The -8.2dBm power will be DC voltage reading and the other two harmonics are negligible. It proves the BPF is necessary and sufficient for the RF signal detector.

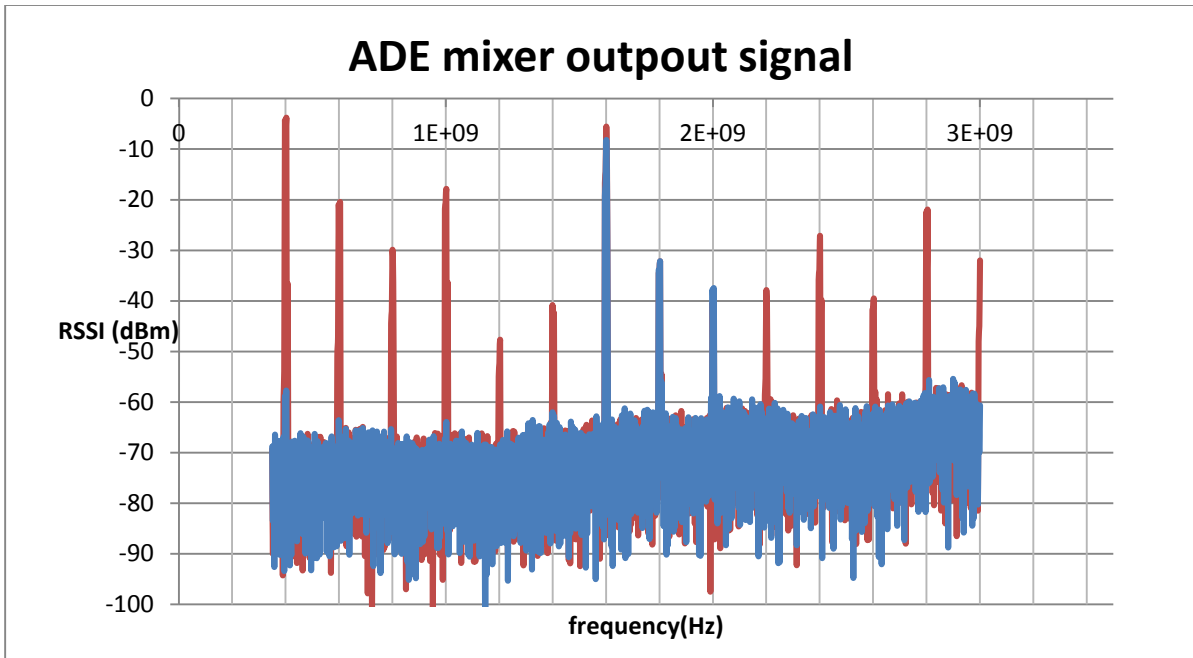


Figure 5.4 BPF filters out unwanted frequencies at 400MHz and out-of-band harmonics



Figure 5.5 shows the actual tests results on the Agilent Spectrum Analyzer. Figure 5.5 also shows that the midfield signal centered at 1.6GHz is -8.14dBm, and the harmonics centered at the 1.8GHz is -28dBm. The harmonics are 20dB less than the midfield power, which is the ratio of  $10^{(-20/10)} = 0.01 = 1\%$ .

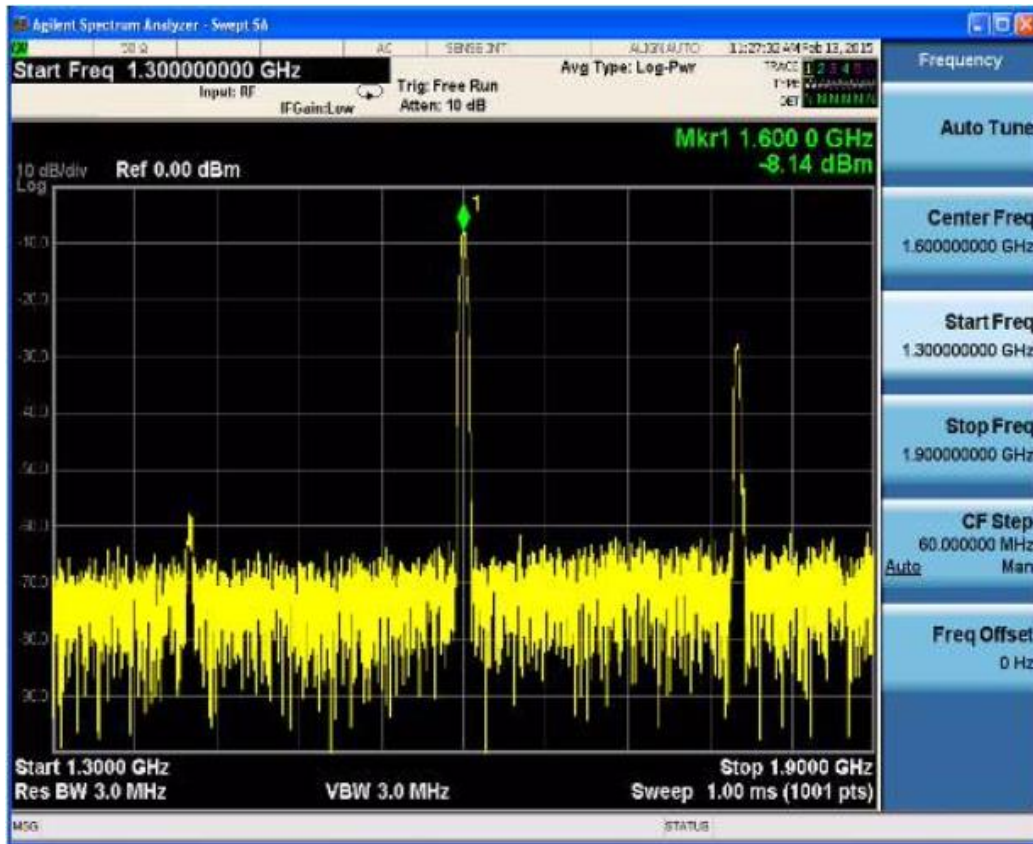


Figure 5.5 Spectrum analyzer midfield power measurement from 1.3 to 1.9GHz

Figure 5.6 shows that the LT5534 RF Detector correctly measured RSSI vs Voltage, showing a slope of 41mV/dB, which agrees with the datasheet specification. The validation test is done and the RF signal generator and Band Pass Filter can be further used for midfield power validation.

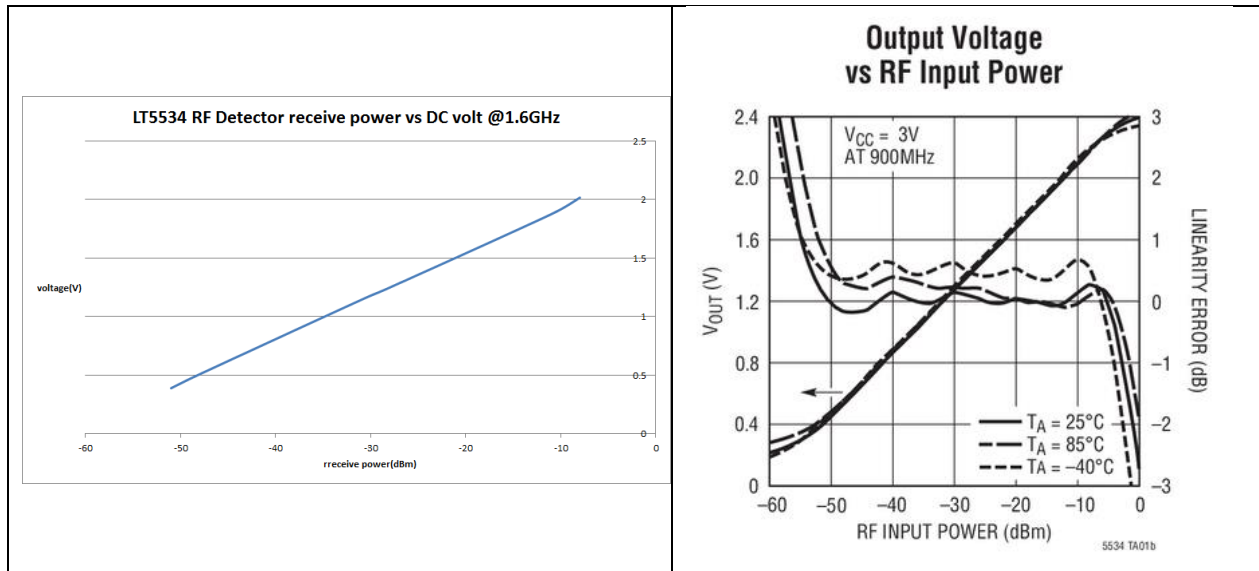


Figure 5.6 LT5534 RF Detector output DC voltage vs. received power

Figure 5.7 shows the voltage-to-RSSI reading conversion platform which converts the LT5534 DC output voltage to the RSSI reading on LCD. The precision is up to two digits.

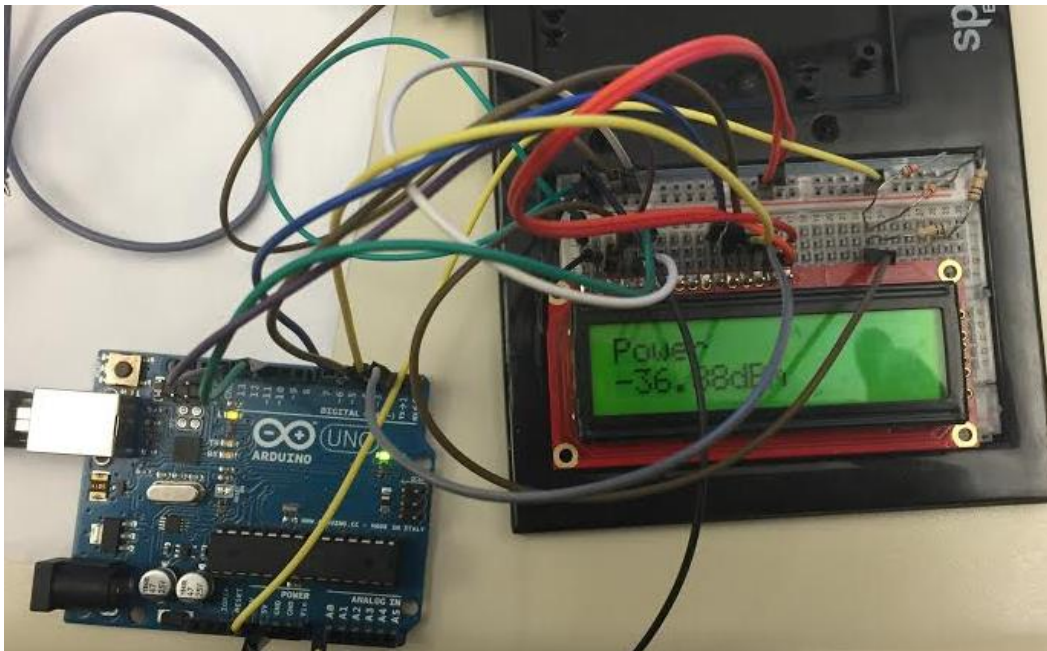


Figure 5.7 RSSI reading on LCD screen using Arduino

## 6. Conclusions and Recommendations

The RF signal Detector takes signal at 1.6GHz and outputs the RSSI reading on LED screen. The mixer does mix a LO signal at 1GHz and an IF signal at 0.6GHz, and output RF signals at 1.6GHz and 0.4GHz and harmonics with a 0.2GHz frequency space. The RF signal detector validation system has a 1.8dB insertion loss, and it linearly converts the RSSI into DC voltage with a 41mV/dB slope, and then the DC voltage is programmed by Arduino to present the RSSI on the LCD screen, as shown in Figure 5.7 in section 5. This system greatly simplifies the Midfield patch validation testing.

For future development, an adjustable attenuation of RSSI measurement is recommended for midfield characterization. Moreover, an integrated mixer with adjustable LO (local oscillator) frequency is recommended for a wideband RF signal detection.

## Bibliography

1. John S. Ho, Sanghoek Kim, S. Y. Poon “Midfield Wireless Powering for Implantable Systems”, May 20, 2013, December 10, 2014
2. A. S. Y. Poon, S. O’Driscoll, and T. H. Meng, “Optimal operating frequency in wireless power transmission for implantable devices,” in Proc. Annu. Int. Conf. IEEE Eng. Med
3. Sanghoek Kim, John S. Ho, and Ads S. Y. Poon “Midfield Wireless Powering of Subwavelength Autonomous Devices”, Feb 20 2013, December 11, 2015
4. John S. Ho, Alexander J. Yeh, Evgenios Neofytou, Sanghoek Kim, Yuji Tanabe, Bhagat Patlolla, Ramin E. Beygu, and Ada S. Y. Poon “Wireless power transfer to deep-tissue micro implants”, April 3, 2014, December 10, 2014.
5. R.F. Harrington, Time-Harmonic Electromagnetic Fields (IEEE, New York, 2011).  
December 10, 2015.
6. IEEE standard for safety with respect to human exposure to radio frequency electromagnetic fields, 3 KHz to 300 GHz, December 5, 2015.
7. W. C. Chew, Waves and Fields in Inhomogeneous Media. Piscataway, NJ, USA: IEEE Press, 1995. December 13 2015.
8. V. Poor, “Robust matched filters,” IEEE Trans. Inf. Theory, vol. IT-29. No. 5, pp. 677-687, Sep. 1983. December 12 2015.
9. E. S. Hochmair, “System optimization for improved accuracy in transcutaneous signal and power transmission,” IEEE Trans. Biomed. Eng., vol. BME-31, no. 2, pp177-186, Feb. 1984. December 10 2015.
10. Danielle Nishida A Wearable 1.6GHz Non-Invasive Midfield Wave-Based Blood Glucose Sensor, March 6 2015, December 11, 2015.

11. Linear Technology LT5534 datasheet December 15, 2014. Online:

<http://cds.linear.com/docs/en/datasheet/5534fc.pdf>